Article

Discovery Medicine 2026; 38(208): 1635–1648
https://doi.org/10.24976/Discov.Med.202638208.128

Hypoxia Bone Marrow Mesenchymal Stem Cell-derived Exosomal AHCY Facilitates the Development of Lung Cancer via MCCC2-activated ERK Pathway

Bing Han[1], Feifei Ma[2,*], Junhua Hu[3], Zhenzhen Zheng[2], Chao Su[4], Xinnan Song[5]

[1]Department of Respiratory Medicine, Jinan Third People's Hospital, 250132 Jinan, Shandong, China
[2]Department of Anesthesiology, Jinan Third People's Hospital, 250132 Jinan, Shandong, China
[3]Department of Neurosurgery, The 990th Hospital of the Joint Logistics Support Force of the Chinese People's Liberation Army, 463002 Zhumadian, Henan, China
[4]Department of Respiratory and Critical Care Medicine, The Third Affiliated Hospital of Shandong First Medical University, 250031 Jinan, Shandong, China
[5]The Fifth Clinical Medical College, Guilin Medical University, 541002 Guilin, Guangxi, China
*Correspondence: mafeifei_mf@163.com (Feifei Ma)
Submitted: 11 December 2025 Revised: 12 March 2026 Accepted: 10 April 2026 Published: 20 May 2026

Background: Bone marrow mesenchymal stem cell-derived exosomes (BMSC-exo) can promote the metastasis of lung cancer (LC) under hypoxic conditions, but the mechanism needs to be explored. This study aims to investigate the role of adenosylhomocysteinase (AHCY) derived from hypoxia BMSC-exo in the development of LC.

Methods: BMSC-exo under normoxic or hypoxic conditions were identified by transmission electron microscope. The relationship between AHCY and methylcrotonyl-CoA carboxylase subunit 2 (MCCC2) was analyzed by bioinformatics analysis. The expression levels of AHCY in hypoxia BMSC-exo or LC cells treated with hypoxia BMSC-exo were determined by quantitative real-time polymerase chain reaction (qRT-PCR). The viability, migration, invasion, and the expression levels of N-cadherin, E-cadherin and extracellular regulated protein kinases (ERK) pathway-related proteins in LC cells transfected with MCCC2 overexpression plasmid and AHCY specific small interfering RNA (siAHCY) as well as treated with normal/hypoxia BMSC-exo were determined using cell counting kit-8 (CCK-8), transwell assay and Western blotting.

Results: AHCY was highly expressed in hypoxia BMSC-exo ($p < 0.001$). With the increase in the exosome release inhibitor GW4869 concentration, the total amount of AHCY protein detected in exosomes isolated from equal volumes of conditioned medium derived from hypoxic BMSCs gradually decreased ($p < 0.001$). Hypoxia BMSC-exo facilitated cell viability, migration, invasion and the expressions of N-cadherin and MCCC2, yet inhibited E-cadherin expression, while these effects were reversed by siAHCY ($p < 0.05$). AHCY and MCCC2 are positively correlated in LC. SiAHCY downregulated the ratio of p-ERK1/2/ERK1/2, whereas this effect was reversed by MCCC2 overexpression ($p < 0.05$).

Conclusions: Hypoxia BMSC-exo carries AHCY to up-regulate MCCC2 expression in LC cells, thereby activating the ERK pathway to facilitate the development of LC. This study identifies a novel exosome-mediated mechanism in the tumor microenvironment and highlights potential therapeutic targets for intervention.

Keywords: lung cancer; adenosylhomocysteinase; methylcrotonyl-CoA carboxylase subunit 2; exosomes; bone marrow mesenchymal stem cells

Introduction

Lung cancer (LC) is a molecular heterogeneous disease with elevated morbidity, high mortality and poor prognosis [1]. Surgical resection is an effective treatment method for early LC, and late-stage LC patients who cannot be treated with surgical resection mostly receive a combination of chemotherapy or radiation therapy [2]. However, LC patients who receive this traditional treatment have a higher proportion of tumor metastasis or recurrence, leading to poor prognosis [3]. Therefore, developing more potent therapeutic modalities is essential to improve the long-term quality of life of LC sufferers.

Due to their involvement in LC development, exosomes can be considered early diagnostic tools for LC [4]. Exosomes are lipid vesicles, approximately 100 nm in diameter, released by cells that carry various functional biomolecules and act as intercellular communication mediators [5]. Bone marrow mesenchymal stem cells (BMSCs) are the main component of the LC microenvironment, possessing self-renewal, multi-directional differentiation potential, and tumor targeting ability [6,7]. BMSC-derived exosomes (BMSC-exo) play dual roles: on one hand, carrying anticancer cargos for tumor suppression; on the other hand, promoting tumor growth [8]. Xina Zhang *et al*. [9]

pointed out that BMSC-exo can promote the metastasis of LC in the LC microenvironment under hypoxic conditions. Hypoxia is a characteristic of LC because the malignant proliferation of LC cells will lead to a lack of oxygen supply, which will lead to local hypoxia [10]. Therefore, exploring the regulatory mechanism of BMSC-exo on LC under hypoxia may be beneficial to improve the cell therapy of LC.

Therefore, we identified 126 genes that were both upregulated in LC and enriched in BMSC-exo by bioinformatics analysis. Among these genes, adenosylhomocysteinase (AHCY) has been related to poor prognosis in LC [11], but the underlying mechanisms remain unclear. In addition, chronic hypoxia has been reported to increase gene expression of AHCY [12]. For these reasons, we chose AHCY for in-depth investigation. Furthermore, we identified 169 genes that were abnormally expressed in LC and differentially expressed in cells treated with an AHCY inhibitor by bioinformatics analysis. Among these genes, methylcrotonyl-CoA carboxylase subunit 2 (MCCC2) was predicted by Gene Expression Profiling Interactive Analysis (GEPIA, http://gepia.cancer-pku.cn/) to be positively correlated with AHCY in lung adenocarcinoma (LUAD) and lung squamous cell carcinoma (LUSC). MCCC2 can promote the activation of the extracellular regulated protein kinases (ERK) pathway [13] and is instrumental in LC progress [14]. Accordingly, we hypothesize that hypoxia BMSC-exo may carry AHCY to LC cells, thereby upregulating MCCC2 expression and promoting the development of LC.

Materials and Methods

Cell Culture

Human BMSCs (AW-PH180, Anweisci, Shanghai, China) were cultured in BMSCs specific medium (SNPM-H096, Sunncell, Wuhan, China), while LC cell lines A549 (AW-CH0021, Anweisci, Shanghai, China) and H125 (YS1163C, YaJi Biological, Shanghai, China) were cultured in F12K medium (AW-M06, Anweisci, Shanghai, China) containing 10% fetal bovine serum (FBS, AW-FBS-001, Anweisci, Shanghai, China) and 1% penicillin streptomycin (SNA-001, Sunncell, Wuhan, China) at 37 °C with 5% CO_2. According to the experimental requirements, BMSCs need to undergo normoxic (20% oxygen) or anoxic (1% oxygen) culture as previously described [15]. Cell lines were routinely tested to confirm the absence of mycoplasma contamination and were authenticated using short tandem repeat (STR) detection.

Isolation of BMSC-exo

Exosomes were isolated as previously described with a few modest adjustments [16]. To remove exosomes, FBS was centrifuged at 100,000 ×g for 16 hours. BMSCs were incubated for 48 hours in medium supplemented with 10% exosome-depleted FBS. Exosomes were isolated by sequential centrifugation, including 1000 ×g for 10 min to remove cells and 8000 ×g for 30 min to clear cellular debris. The supernatant was filtered through a 0.22 μm filter and further ultracentrifuged at 130,000 ×g for 70 min. The precipitate was then resuspended in phosphate-buffered saline (PBS, C0221B, Beyotime, Shanghai, China) and centrifuged again to obtain the precipitate (BMSC-exo).

Identification of BMSC-exo

Employing a transmission electron microscope (TEM, HT7800, HITACHI, Tokyo, Japan), exosome morphology was investigated. Simply said, the phosphotungstic acid solution (D6035, Nobleryder, Beijing, China) was dripped on the copper net after the exosome suspension was dropped there to stain it. Exosomes were then observed and imaged using TEM after the samples were air-dried under an incandescent lamp. Additionally, CD63 Molecule (CD63) and Tumour Susceptibility Gene 101 (TSG101), which are exosome-specific markers, were identified using Western blotting.

Transfection

MCCC2 overexpression plasmid (oe-MCCC2, pCDNA3.1(+)-Flag-MCCC2, OBiO Technology, Shanghai, China) and its corresponding empty-vector plasmid as the negative control (NC, HG-VPI0001, HonorGene, Changsha, China) were prepared. **Supplementary File 1** exhibited the CDS sequence of MCCC2. AHCY-specific small interfering RNA (siAHCY, sense: 5′-CUGACAAACUGCCCUACAA-3′; antisense: 5′-UUGUAGGGCAGUUUGUCA-3′) and siNC (sense: 5′-CCUACGCCACCAAUUUCGU-3′; antisense: 5′-ACGAAAUUGGUGGCGUAGG-3′) were provided by GENERAL BIOL (Chuzhou, China). The lipid-based method was used to transfect cells with the plasmid constructs. For transfection, 500 ng siRNA or overexpression plasmid was transfected into 1.3 × 10^5 cells in 24-well plates using Lipofectamine 3000 (L3000150; Thermo Fisher, Waltham, MA, USA). The cells were cultured to reach an 80%–90% confluence. Opti-MEM media (25 μL) and Lipofectamine 3000 transfection reagents (1.5 μL) were put into an Eppendorf tube. Opti-MEM media (25 μL), P3000 reagents (1 μL), and siRNA or overexpress plasmids (0.5 μL) were added to another Eppendorf tube. Then, the two tubes were gently mixed, followed by incubation with siRNA or plasmids for 10 min at room temperature. 50 μL of the above mixture was added to the cell. The cells were incubated for 48 h at 37 °C. Transfection efficiency was evaluated by quantitative real-time polymerase chain reaction (qRT-PCR).

Table 1. Primers used in this study.

Genes	5′–> 3′
AHCY (Human) F	CGGGAAAGGAGAGACCCCTA
AHCY (Human) R	TTGCTCTTGGTGACGGAGTC
MCCC2 (Human) F	ACGCAAGCAGGGTACCATTT
MCCC2 (Human) R	TCTTAGGCACTTGGGCACAG
β-actin (Human) F	CATGTACGTTGCTATCCAGGC
β-actin (Human) R	CTCCTTAATGTCACGCACGAT

Abbreviation: *AHCY*, adenosylhomocysteinase; *MCCC2*, methylcrotonyl-CoA carboxylase subunit 2; F, Forward; R, Reverse.

Grouping

In the first part, 5 or 10 µM of GW4869 (exosomes release inhibitor, HY-19363, MedChemExpress, Shanghai, China) was added to the medium before BMSCs were treated with anoxic conditions for 48 hours. Exosomes were then isolated from equal volumes of conditioned media harvested from an equal number of cells across all groups. This ensured that any difference in the amount of AHCY detected was attributable to the effect of GW4869 on exosome secretion.

In the second part, A549 and H125 cells were assigned into five groups: control (PBS treatment and normal culture), normal BMSC-exo (BMSC-exo treatment under normoxia for 48 hours), hypoxia BMSC-exo (BMSC-exo treatment under anoxia for 48 hours), siNC (treatment of exosomes from siNC-transfected BMSCs under anoxia for 48 hours) and siAHCY (treatment of exosomes from siAHCY-transfected BMSCs under anoxia for 48 hours).

In the third part, there were four groups: hypoxia BMSC-exo (the same as the above- mentioned), siNC+NC, siAHCY+NC and siAHCY+MCCC2. A549 and H125 cells in the latter three groups were co-transfected with siNC/siAHCY and NC/oe-MCCC2, followed by treatment with exosomes isolated from BMSCs under anoxia for 48 hours.

qRT-PCR

Total RNA was extracted with exosome RNA extraction kit (abs60263, absin, Shanghai, China) or Trizol reagent (2101, Genenode, Wuhan, China). Reverse transcription kit (E3010, NEB, Ipswich, MA, USA) was applied to synthesize complementary DNA (cDNA) from RNA. The resulting cDNA was mixed with primers (Table 1) and qPCR Mix (M3003, NEB, Ipswich, MA, USA) for qPCR analysis on the instrument (Fascan 48E, Tianlong, Xi'an, China). For all gene expression analyses, cells were harvested at approximately 80–90% confluence to ensure consistency in cell number and physiological state across treatment groups. Total RNA was extracted from an equal number of culture wells under identical conditions. AHCY and MCCC2 relative expression levels were calculated using the $2^{-\Delta\Delta CT}$ method and normalized by β-actin.

Endocytosis of BMSC-exo

Diluent C (1 mL, MX4022, MaoKangBio, Shanghai, China) was used to dilute BMSC-exo and PKH67 (C2073S, Beyotime, Shanghai, China), respectively. Then the diluted BMSC-exo and PKH67 were mixed for 5-minute cultivation, which was terminated by 2 mL bovine serum albumin (BSA, MP6105, MaoKangBio, Shanghai, China). The BMSC-exo was suspended in PBS and added to LC cells, and incubated for 5 hours. The cells were fixed with 4% paraformaldehyde (P0099, Beyotime, Shanghai, China) and the nuclei were colored with 4′,6-diamidino-2-phenylindole (DAPI, MX4209, MaoKangBio, Shanghai, China). Residual dye was eliminated by washing with PBS prior to fluorescence microscopy analysis (WMF-3580, Shyuguang, Shanghai, China).

Cell Counting Kit-8 (CCK-8)

Utilizing the CCK-8 kit (C0037, Beyotime, Shanghai, China), cell viability was assessed. In 96-well plates, LC cells (3000/well) were cultured for 24, 48 or 72 hours, followed by incubation with CCK-8 solution for 2 hours. The wavelength (450 nm) was determined using a microplate reader (HBS-ScanX, Detie, Nanjing, China).

Transwell Assay

To evaluate the invasive and migratory capacities of LC cells, Transwell inserts were pre-coated with or without Matrigel (354262, Corning, Corning, NY, USA). LC cells suspended in serum-free medium were added to the upper chamber. Medium containing 20% FBS was added to the lower chamber. 24 hours later, cells on the upper side of the insert were removed with a cotton swab. Cells on the lower side were fixed (4% paraformaldehyde) and stained (0.1% crystal violet; WKQ-0007202, Weikeqi-biotech, Chengdu, China). Results were observed using an inverted microscope (N300M, Yongxin, Ningbo, China).

Western Blotting

Lysis solutions of LC cells were generated via the radio immunoprecipitation assay lysis buffer (RIPA) (WB9202, Bio-swamp, Wuhan, China). Proteins were placed into sodium dodecyl sulfate-polyacrylamide gel electrophoresis (SDS-PAGE) gel (P0818, Nobleryder, Beijing, China) after being measured by the bicinchoninic acid assay (BCA) Protein Assay kit (BBCAPCK500, Bioswamp, Wuhan, China). After electrophoresis, proteins were transferred onto a polyvinylidene fluoride membrane (PVDF, MF452, Mei5bio, Beijing, China), followed by blocking with 5% BSA. Primary and secondary antibodies were employed to incubate proteins (Table 2). Protein bands were detected using an enhanced chemiluminescence (ECL) kit (P0018S, Beyotime, Shanghai, China) and visualized with an imaging system (SynGene, Frederick, MD, USA). Band intensities were quantified using ImageJ software (version 1.41, National Institutes of Health, Bethesda,

Table 2. Antibodies used in this study.

Name	Catalog	Molecular weight	Dilution	Manufacturer
CD63	ab271286	26 kDa	1/1000	abcam, Cambridge, UK
MCCC2	12117-1-AP	61 kDa	1/1000	Proteintech, Wuhan, China
TSG101	ab30871	49 kDa	1/1000	abcam, Cambridge, UK
GM130	ab169276	83 kDa	1/1000	abcam, Cambridge, UK
AHCY	ab134966	47 kDa	1/1000	abcam, Cambridge, UK
N-cadherin	ab18203	130 kDa	1/1000	abcam, Cambridge, UK
E-cadherin	ab40772	97 kDa	1/1000	abcam, Cambridge, UK
p-ERK1/2	#9101	44/42 kDa	1/1000	CST, Boston, DA, USA
ERK1/2	#4695	44/42 kDa	1/1000	CST, Boston, DA, USA
β-actin	ab8226	42 kDa	1/1000	abcam, Cambridge, UK
goat anti rabbit	ab205718	—	1/2000	abcam, Cambridge, UK
goat anti mouse	ab205719	—	1/2000	abcam, Cambridge, UK

Abbreviation: CST, cell signaling technology.

MD). The target protein gray value/β-actin gray value was used as the relative protein expression. The relative protein level was normalized to the control group. β-actin was used as the internal reference protein.

Bioinformatics Analysis

Using the GEO2R online tool to analyze the dataset GSE18842, with the threshold of adjusted p value $<$ 0.05 and log2FC $>$1, 1416 genes significantly upregulated in lung cancer were selected. Subsequently, 938 human mesenchymal stem cell exosomal proteins were obtained from the ExoCarta database (http://www.exocarta.org/). Then, the intersection of the two was obtained using the BioVenn online tool, yielding 126 common genes, among which AHCY was selected for subsequent experiments. To explore the downstream targets of AHCY, we analyzed the GSE17589 dataset (cells treated with AHCY inhibitor), identifying 684 differentially expressed genes using the same threshold. These genes were then intersected with LC-related differentially expressed genes from the GSE18842 dataset (3196 genes), resulting in 169 overlapping genes. From this subset, MCCC2 was selected for subsequent verification. Finally, correlation analysis was performed using the GEPIA web network (http://gepia.cancer-pku.cn/). In the "Correlation Analysis" module, AHCY and MCCC2 were entered as target genes, and "LUAD" and "LUSC" datasets were selected. The platform automatically calculated and reported the Pearson correlation coefficient (R) and p value.

Statistical Analysis

The experiments were triplicate (n = 3 biological replicates). The Shapiro-Wilk test was used to verify the normality of the data distribution, and the Levene test was performed to assess the homogeneity of variances prior to statistical analysis. The comparison between the two groups was conducted using the independent sample t-test, while the comparisons among multiple groups were performed using one-way analysis of variance (ANOVA), and the Tukey test was applied for post hoc comparisons. All experimental results were analyzed using SPSS 21.0 system (SPSS Inc., Chicago, DE, USA) and expressed as the Mean $\pm$ standard deviation (SD). $p < 0.05$ was considered statistically significant.

Results

AHCY Was Highly Expressed in Hypoxia BMSC-exo

Exosomes were isolated from BMSCs cultured with 20% oxygen (normal condition) or 1% oxygen (hypoxic), and were designated as normal BMSC-exo or hypoxia BMSC-exo. The morphology of normal BMSC-exo and hypoxia BMSC-exo was observed through a TEM (Fig. 1A). The appearance, size, and basic characteristics of both exosome groups remained consistent. CD63 and TSG101 were expressed in exosomes derived from BMSCs under both incubation conditions, but not contain GM130 expression (Fig. 1B). Fig. 1C displayed the intersection of upregulated genes (1416) in LC obtained from the GSE18842 dataset and extracellular proteins (938) derived from mesenchymal stem cells obtained from ExoCarta (http://www.exocarta.org/). Among the 126 intersecting genes, AHCY was selected for further study. Notably, AHCY was highly expressed in hypoxia BMSC-exo in comparison with the normal BMSC-exo group (Fig. 1D, $p < 0.001$). Additionally, isolation of exosomes from equal volumes of conditioned media revealed that GW4869 treatment led to a concentration-dependent reduction in the AHCY mRNA levels detected in the exosome fraction (Fig. 1E, $p < 0.001$).

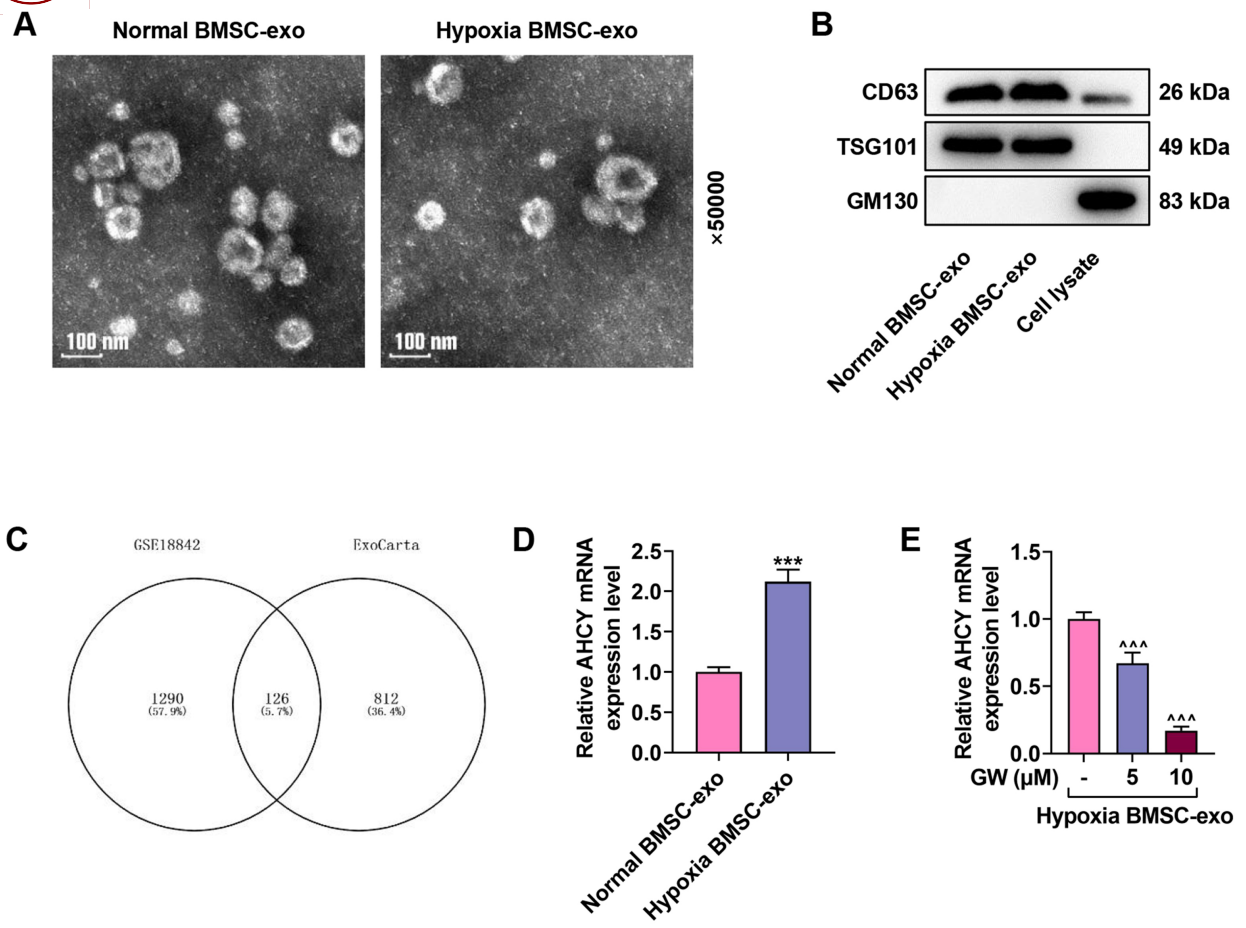

Fig. 1. Identification of BMSC-exo and the expression level of AHCY in BMSC-exo. (A) Exosome morphology (transmission electron microscope). Scale bar = 100 nm. Magnification, 50,000×. (B) Specific exosome surface markers (CD63, TSG101, and GM130) in BMSCs-derived exosomes (BMSC-exo) (Western blotting). (C) Intersection of upregulated genes in lung cancer obtained from the GSE18842 dataset and extracellular proteins from mesenchymal stem cells obtained from ExoCarta (http://www.exocarta.org/) (Venn diagram). (D) BMSCs were cultured with 20% oxygen (normoxic) or 1% oxygen (hypoxic), and exosomes were isolated from 5 $\times$ 10^9 BMSCs under normoxia or anoxia. AHCY expression in normal BMSC-exo or hypoxia BMSC-exo (qRT-PCR, β-actin as internal control). (E) GW4869 (exosomes release inhibitor, 5, 10 μM) was added to the medium before BMSCs were put in hypoxic chamber. AHCY expression in hypoxia BMSC-exo (qRT-PCR, β-actin as internal control). ***$p < 0.001$ vs. normal BMSC-exo. $^{\wedge\wedge\wedge}p < 0.001$ vs. hypoxia BMSC-exo. The experiments were triplicate (n = 3 biological replicates). qRT-PCR, quantitative real-time polymerase chain reaction; BMSCs, Bone marrow-derived mesenchymal stem cells; AHCY, adenosylhomocysteinase.

SiAHCY Reversed the Effects of Hypoxia BMSC-exo on Viability, Migration, Invasion and Epithelial-mesenchymal Transition (EMT) of LC Cells

Fluorescence microscope demonstrated that both normal BMSC-exo and hypoxia BMSC-exo were effectively internalized by LC cells (Fig. 2A). To unveil how BMSC-exo impacts LC cell malignant development, exosomes derived from transfected/untransfected siNC/siAHCY and hypoxic cultured BMSCs were used to treat A549 and H125 cells. AHCY expression in exosomes isolated from BMSCs which transfected with siAHCY was lower than in the exosomes isolated from BMSCs which transfected with siNC, indicating the transfection was successful (Fig. 2B–D, $p <$ 0.001).

Further, the cells were divided into five groups: control (A549 and H125 cells were treated with PBS), normal BMSC-exo (A549 and H125 cells were treated with exosomes isolated from BMSCs under normoxia), hypoxia BMSC-exo (A549 and H125 cells were treated with exosomes isolated from BMSCs under anoxia), siNC (A549 and H125 cells were treated with exosomes isolated from BMSCs which transfected with siNC under anoxia) and siAHCY (A549 and H125 cells were treated with exosomes isolated from BMSCs which transfected with siAHCY under anoxia). Analysis of the recipient LC cells revealed that AHCY expression was higher in the Normal BMSC-exo treatment, compared with the Control group. This increase was further augmented in cells treated with hypoxic BMSC-exo. Conversely, the siAHCY group effec-

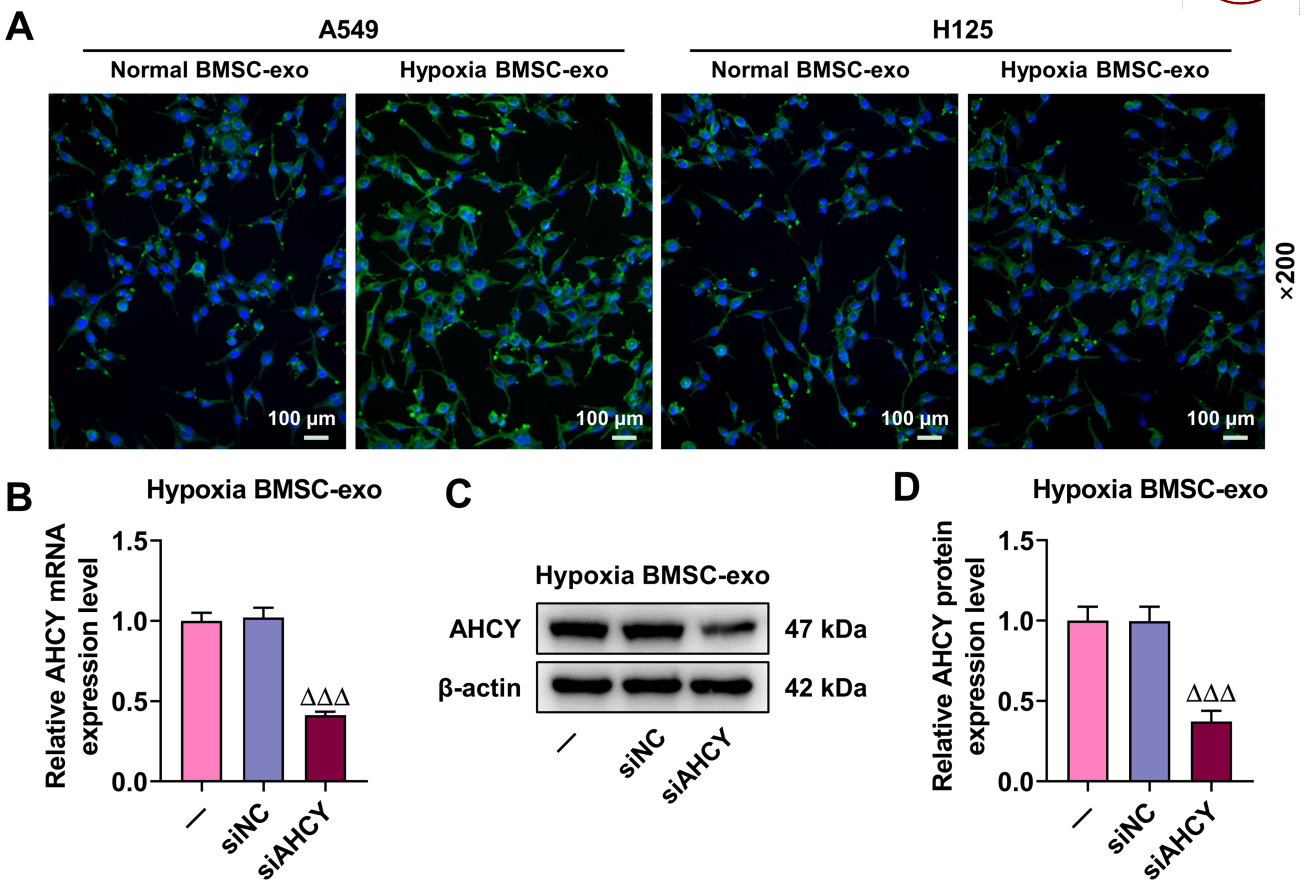

Fig. 2. The effects of hypoxia BMSC-exo and siAHCY on AHCY expression of LC cells. (A) Uptake of PKH67-labelled normoxic EVs or hypoxic EVs (20 μg/mL) by A549 and H125 cells (scale bar = 100 μm, scale bar = 200×). (B–D) AHCY expression in LC cells (qRT-PCR and Western blotting, β-actin as internal control). $^{\Delta\Delta\Delta}p < 0.001$ vs. siNC. The experiments were triplicate (n = 3 biological replicates). SiAHCY, AHCY-specific small interfering RNA.

tively reduced AHCY expression compared to the siNC group (Fig. 3A–F, $p < 0.001$). Moreover, the viability (Fig. 3G,H, $p < 0.05$), invasion (Fig. 4A,C,D, $p < 0.01$), and migration (Fig. 4B,E,F, $p < 0.05$) of LC cells were significantly enhanced by treatment with normal BMSC-exo compared to the control. Hypoxic BMSC-exo treatment induced an even stronger promotive effect, whereas AHCY knockdown (siAHCY) decreased the pro-malignant phenotypes (Fig. 3G,H, Fig. 4A–F, $p < 0.05$). In addition, LC cells that ingested normal BMSC-exo expressed more N-cadherin and less E-cadherin than LC cells that added PBS (Fig. 5A–F, $p < 0.05$). LC cells ingesting hypoxia BMSC-exo expressed more N-cadherin and less E-cadherin than LC cells ingesting normal BMSC-exo (Fig. 5A–F, $p < 0.05$). LC cells that ingested siAHCY-transfected hypoxia BMSC-exo express less N-cadherin and more E-cadherin than LC cells that ingested siNC-transfected hypoxia BMSC-exo (Fig. 5A–F, $p < 0.001$).

The Relationship Between AHCY and MCCC2 in LC

Fig. 6A depicts the intersection of the differentially expressed genes (3196) of LC obtained from GSE18842 and the differentially expressed genes (684) of cells treated with AHCY inhibitor obtained from GSE17589. Among the 169 intersecting genes, MCCC2 was selected for further study. According to the prediction of GEPIA website (Fig. 6B,C), a weak yet statistically significant positive correlation was observed between AHCY and MCCC2 in LUSC ($r = 0.18$, $p = 7.6 \times 10^{-5}$) and LUAD ($r = 0.18$, $p = 7.5 \times 10^{-5}$). Interestingly, MCCC2 expression was increased following normal BMSC-exo treatment compared to the control, and was further elevated due to hypoxic BMSC-exo treatment. Conversely, knockdown of AHCY in the BMSCs cells (siAHCY group) effectively reversed this increase, resulting in lower MCCC2 expression (Fig. 6D,E, $p < 0.001$).

MCCC2 Overexpression Reversed the Effects of siAHCY on Viability, EMT and ERK1/2 Pathway in LC Cells Co-cultured With Hypoxia BMSC-exo

To investigate the causal relationship between AHCY and MCCC2 in the malignant development of LC, LC cells were co-transfected with siAHCY and oe-MCCC2 before incubation with hypoxia BMSC-exo. The cells were divided into four groups: hypoxia BMSC-exo (A549 and H125 cells were treated with exosomes isolated from

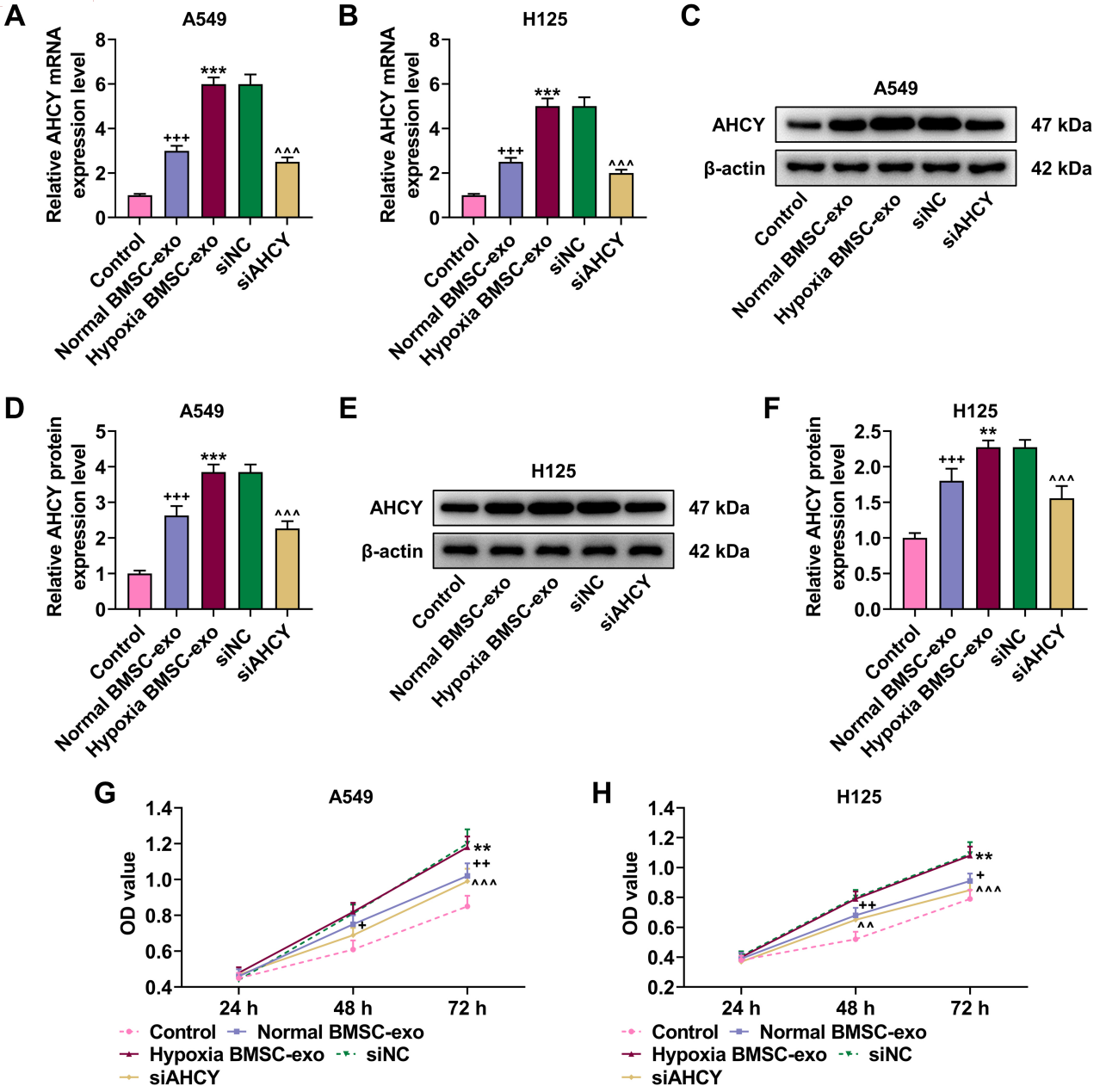

Fig. 3. The effects of hypoxia BMSC-exo and siAHCY on AHCY expression and viability of LC cells. (A–F) AHCY expression in LC cells (qRT-PCR and Western blotting, β-actin as internal control). (G,H) LC cell viability (cell counting kit-8). $^{**}p < 0.01$, $^{***}p < 0.001$ vs. normal BMSC-exo. $^{+}p < 0.05$, $^{++}p < 0.01$, $^{+++}p < 0.001$ vs. Control. $^{\wedge\wedge}p < 0.01$, $^{\wedge\wedge\wedge}p < 0.001$ vs. siNC. The experiments were triplicate (n = 3 biological replicates). SiAHCY, AHCY-specific small interfering RNA.

BMSCs under anoxia), siNC+NC (A549 and H125 cells co-transfected with siNC and NC were treated with exosomes isolated from BMSCs under anoxia), siAHCY+NC (A549 and H125 cells co-transfected with siAHCY and NC were treated with exosomes isolated from BMSCs under anoxia) and siAHCY+MCCC2 (A549 and H125 cells co-transfected with siAHCY and MCCC2 overexpression plasmid were treated with exosomes isolated from BMSCs under anoxia). SiAHCY reduced the expression of AHCY and MCCC2 in LC cells co-cultured with hypoxia BMSC-exo, while this trend was reversed by oe-MCC2 (Fig. 7A–J, $p < 0.05$). Further, the expression of MCCC2 was increased in the siAHCY+MCCC2 group compared with siAHCY+NC, indicating the transfection was successful (Fig. 7A–J, $p < 0.05$). Additionally, siAHCY reduced cell viability (Fig. 7K,L, $p < 0.05$), upregulated E-cadherin, and downregulated N-cadherin and p-ERK1/2/ERK1/2 ratio (Fig. 8A–J, $p < 0.01$) in LC cells co-cultured with hypoxia BMSC-exo, whereas these effects were all reversed by oe-MCC2 (Fig. 7K,L and Fig. 8A–J, $p < 0.05$).

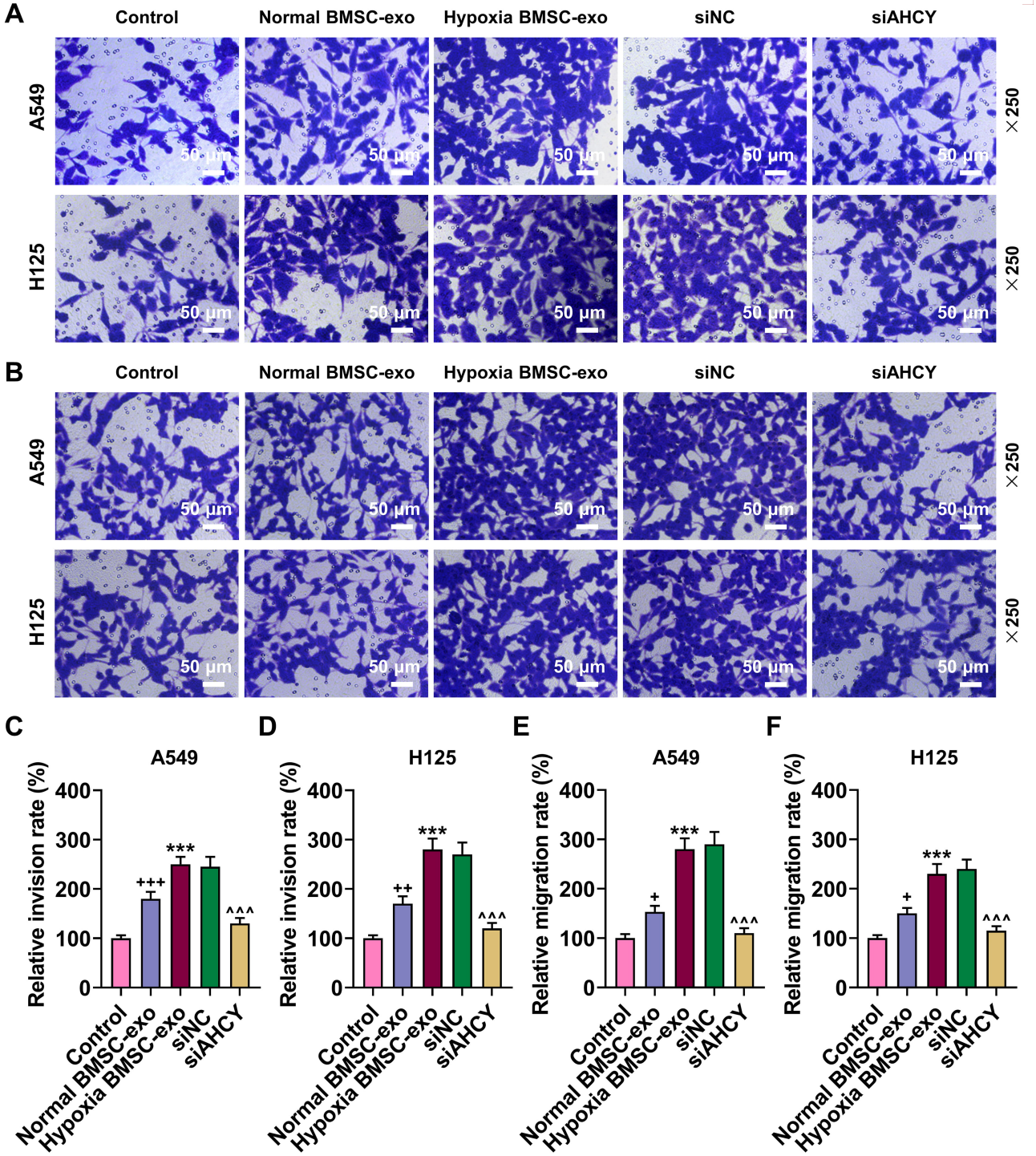

Fig. 4. The effects of hypoxia BMSC-exo and siAHCY on the migration and invasion of LC cells. (A,B) Cell invasion (A) and migration (B) (transwell assay; magnification, 250×, scale bar = 50 μm). (C,D) Quantitation results of cell invasion. (E,F) Quantitation results of cell migration. ***$p < 0.001$ vs. normal BMSC-exo. $^{+}p < 0.05$, $^{++}p < 0.01$, $^{+++}p < 0.001$ vs. Control. $^{\wedge\wedge\wedge}p < 0.001$ vs. siNC. The experiments were triplicate (n = 3 biological replicates).

Discussion

AHCY is related to cellular stress response, which plays an important role in cellular homeostasis and tissue damage [17]. AHCY seems to play a carcinogenic role in cancer cells. Reportedly, AHCY upregulation was detected in colon cancer, which is related to the oxidative stress of cancer cells [18]. Hypoxia represents a cellular stress condition. Our research demonstrated that BMSC-exo can exhibit increased AHCY under hypoxic conditions, and these BMSC-exos can be absorbed by LC cells, thus increasing AHCY (protein/mRNA) expression in LC cells. Further re-

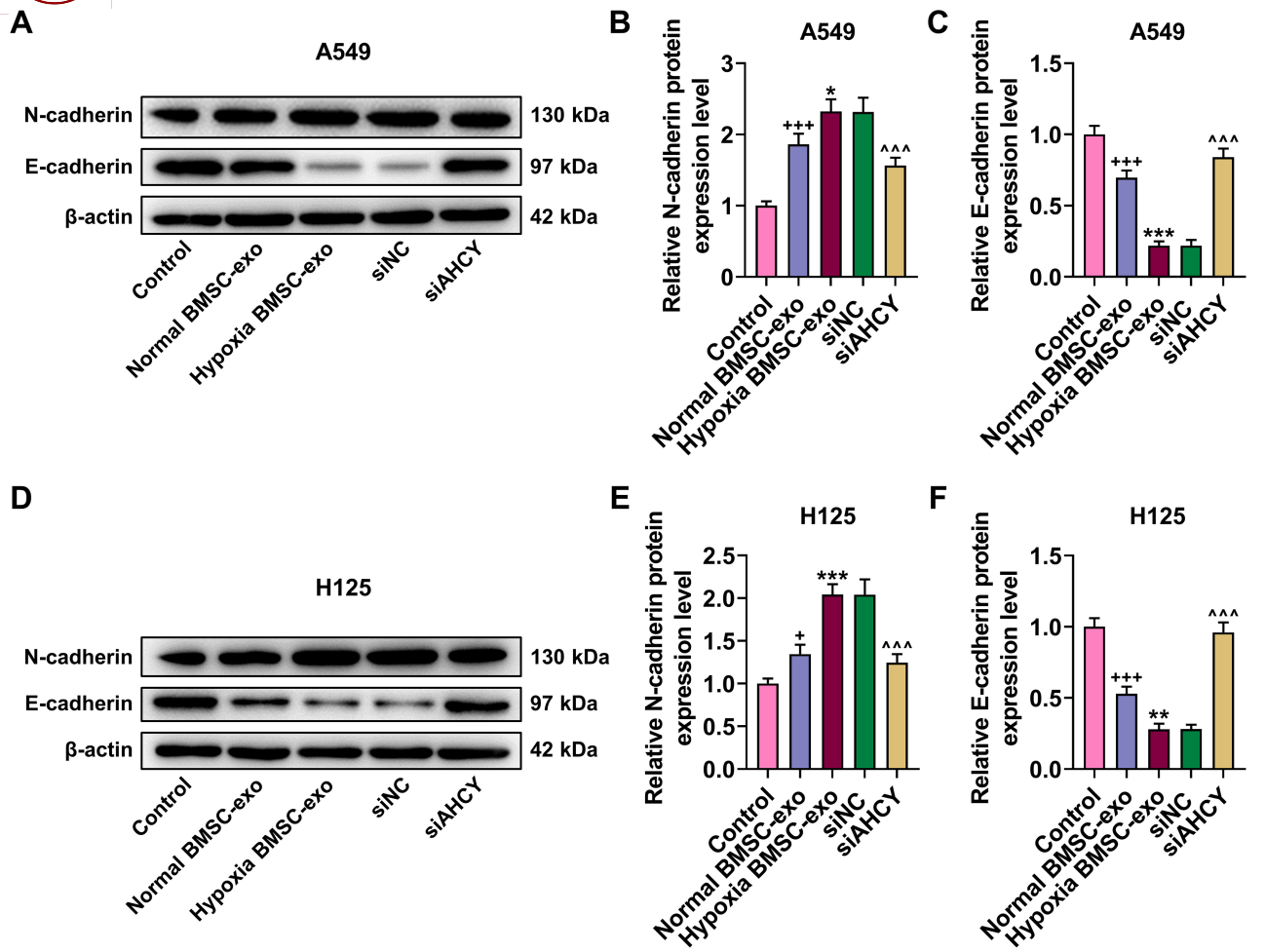

Fig. 5. Effects of exosomes secreted by hypoxia-treated BMSCs transfected with siAHCY on the expression levels of N-cadherin and E-cadherin in LC cells. (A–F) N-cadherin and E-cadherin expression levels in LC cells (Western blotting, β-actin as internal control). $^{*}p < 0.05$, $^{**}p < 0.01$, $^{***}p < 0.001$ vs. normal BMSC-exo. $^{+}p < 0.05$, $^{+++}p < 0.001$ vs. Control. $^{\wedge\wedge\wedge}p < 0.001$ vs. siNC. The experiments were triplicate (n = 3 biological replicates).

search revealed that hypoxia BMSC-exo promotes the malignant phenotype of LC cells, an effect that was reversed by siAHCY. A study has shown that AHCY inhibition can suppress cell proliferation and metastasis by regulating the cell cycle [19]. Therefore, the reason why hypoxia BMSC-exo leads to the malignant development of LC may be related to the upregulation of AHCY expression. On the other hand, AHCY is the only enzyme in mammals that can catalyze the reversible cleavage of S-adenosylhomocystine (SAH), a by-product of methyltransferase activity and an effective inhibitor [17]. Therefore, ACHY can facilitate methylation process. Moreover, Aakriti Gupta and his colleagues also found that AHCY can regulate gene methylation under hypoxia [20]. Therefore, the downstream mechanism of AHCY in LC was further investigated.

After bioinformatics analysis, we found a positive correlation between MCCC2 and AHCY in LC. MCCC2 belongs to the MCC family, and MCC promotes the catabolism of leucine [21]. Leucine may be an essential amino acid for the survival of certain cancer cells [13]. Therefore, the accumulated research reports that the high expression of MCCC2 indicates the poor prognosis of colorectal cancer and breast cancer [22,23]. In our study, LC cells that ingested hypoxia BMSC-exo exhibited higher levels of MCCC2, whereas this trend was reversed by siAHCY, indicating that LC cells may have increased their own MCCC2 expression due to AHCY from BMSC-exo. Although the role of MCCC2 in LC cells remains poorly characterized, MCCC2 has been shown to promote proliferation, migration, and invasion in prostatic cancer cells [24]. Consistently, we found that MCCC2 overexpression reversed the regulatory effects of siAHCY on LC cell viability and EMT, indicating that the reason for the malignant development of LC caused by hypoxia BMSC-exo may be related to the promotion of MCCC2 expression in LC cells through AHCY.

Next, we evaluated the effects of AHCY and MCCC2 on the ERK pathway. The activation of ERK1/2 is considered a marker of cancer because the ERK pathway can regulate cancer cell proliferation and survival [25]. In ad-

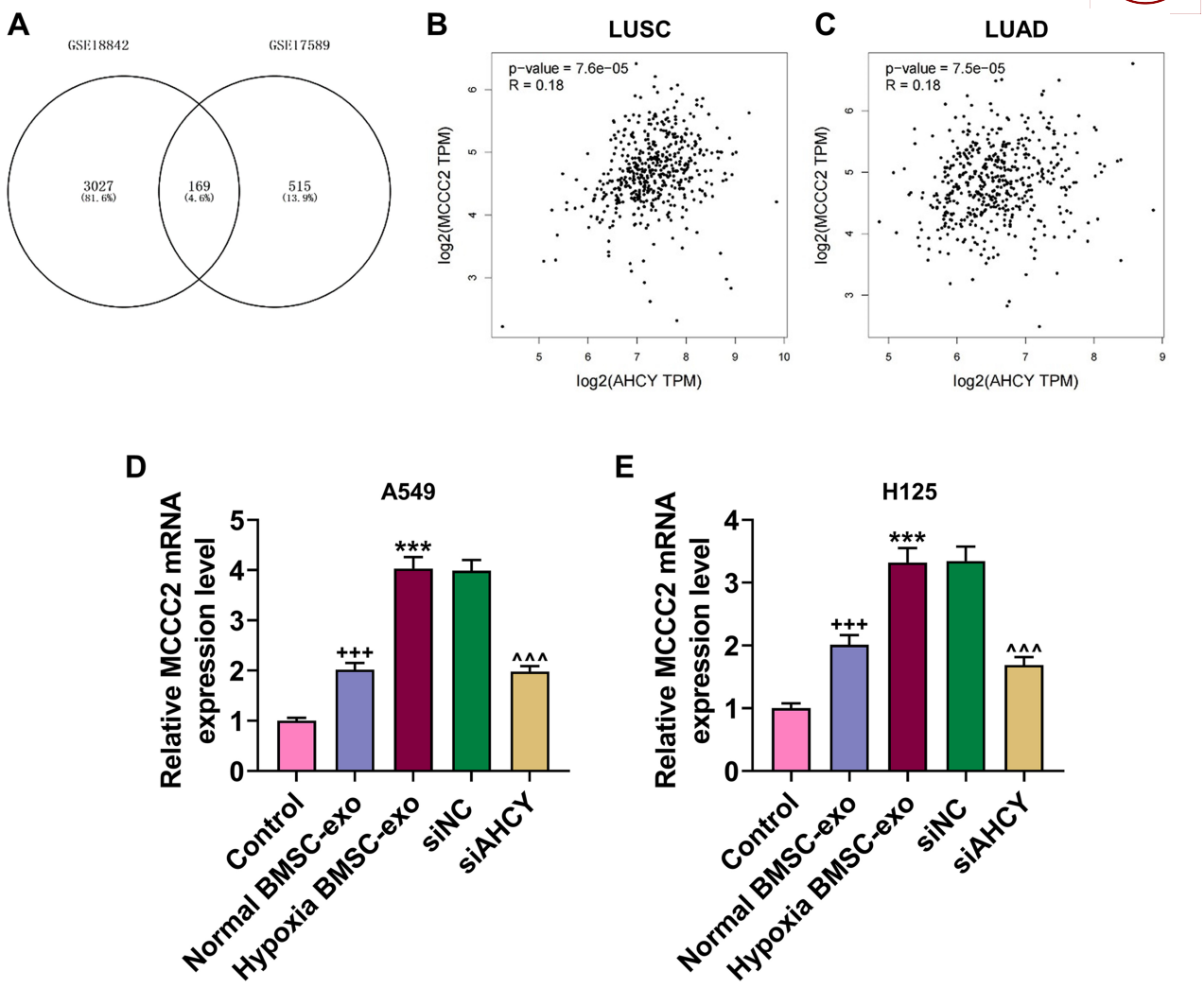

Fig. 6. The relationship between AHCY and MCCC2. (A) Intersection of the differentially expressed genes of cells treated with AHCY inhibitor obtained from GSE17589 and the differentially expressed genes of lung cancer obtained from GSE18842 (Venn diagram). (B) Positive correlation between AHCY and MCCC2 in LUSC (GEPIA). r = 0.18, $p = 7.6 \times 10^{-5}$. (C) Positive correlation between AHCY and MCCC2 in LUAD (GEPIA). r = 0.18, $p = 7.5 \times 10^{-5}$. (D,E) MCCC2 expression in LC cells (qRT-PCR, β-actin as internal control). ***$p < 0.001$ vs. normal BMSC-exo. $^{+++}p < 0.001$ vs. Control. $^{\wedge\wedge\wedge}p < 0.001$ vs. siNC. The experiments were triplicate (n = 3 biological replicates). MCCC2, methylcrotonyl-CoA carboxylase subunit 2.

dition, activating ERK1/2 can also regulate the expression of various proteins in EMT [26], such as N-cadherin and E-cadherin, which were also found to be regulated by siAHCY and oe MCCC2. Sae Jeong Park *et al.*'s study [19] showed that AHCY downregulation can suppress cell proliferation by regulating the MEK/ERK pathway. MCCC2 boosts hepatocellular carcinoma progression via activating the ERK pathway [13]. Similarly, we found that siAHCY inactivated the ERK pathway in LC cells, while this trend was reversed by MCCC2 overexpression, indicating that AHCY may activate the ERK pathway in LC cells by upregulating MCCC2.

Some limitations still exist in this study. Firstly, while our exosome characterization included TEM and specific protein markers, quantitative analysis of particle size distribution (e.g., by NTA) was not performed. Secondly, from a bioinformatics perspective, due to the lack of publicly available transcriptomic data from lung cancer cells treated with AHCY inhibitors, we referred to the GSE17589 dataset (breast cancer cells with DZNep treatment) to screen for potential AHCY-regulated genes, under the assumption that AHCY-mediated transcriptional responses may be partially conserved across cancer types. To enhance lung cancer relevance, we intersected these genes with differentially expressed genes from the lung cancer dataset GSE18842, ultimately identifying MCCC2. However, we acknowledge that cross-cancer analysis has inherent limitations, and the bioinformatics results are hypothesis-generating. The subsequent functional validation in lung cancer cells is therefore essential, and future studies using AHCY inhibitors or genetic manipulation specifically in lung cancer cells followed by transcriptome sequencing are warranted

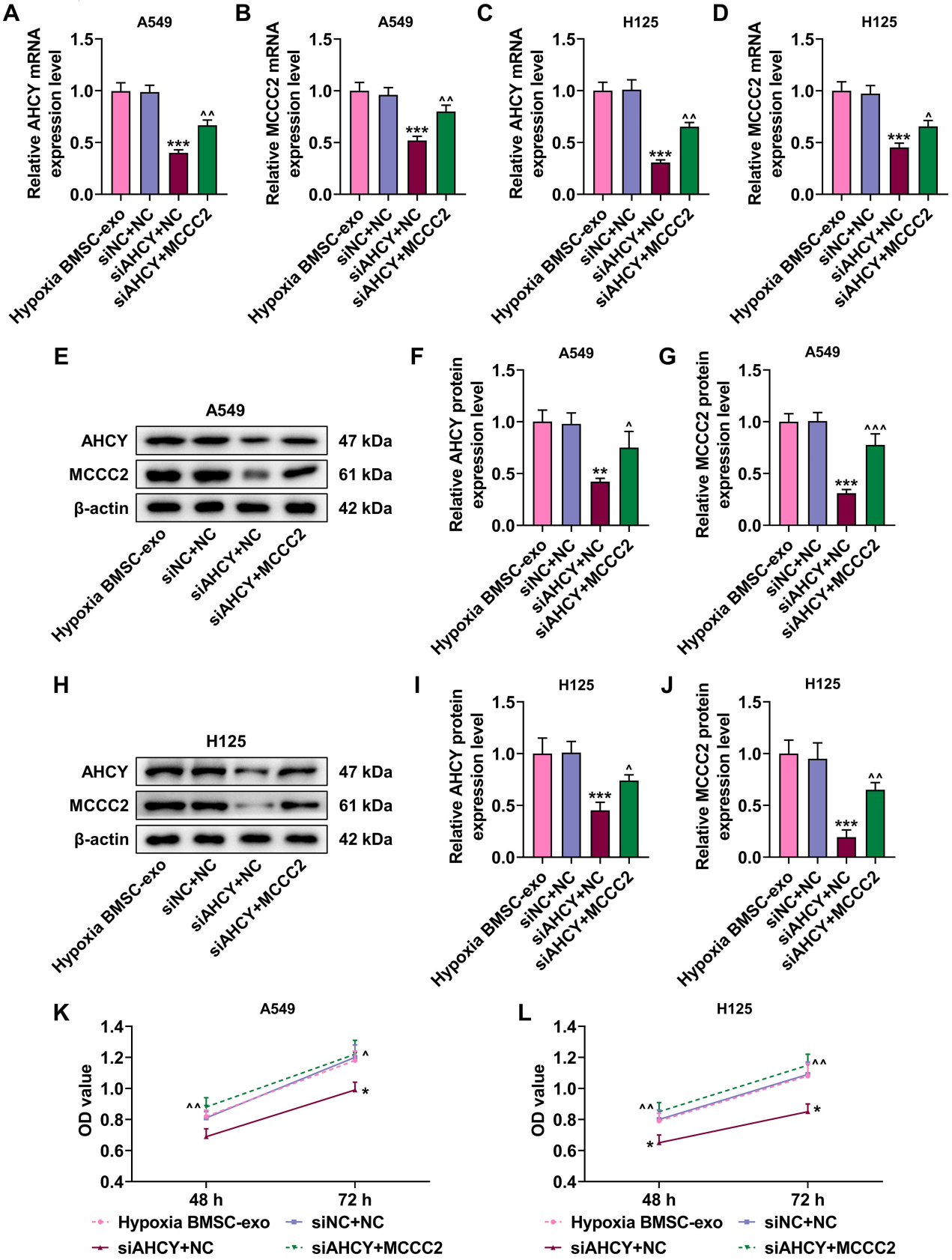

Fig. 7. The effects of siAHCY and MCCC2 overexpression on MCCC2 expression and viability of LC cells. (A–J) AHCY and MCCC2 expression levels in LC cells (qRT-PCR and Western blotting, β-actin as internal control). (K,L) Cell viability (cell counting kit-8). *$p < 0.05$, **$p < 0.01$, ***$p < 0.001$ vs. siNC+NC. ^$p < 0.05$, ^^$p < 0.01$, ^^^$p < 0.001$ vs. siAHCY+NC. The experiments were triplicate (n = 3 biological replicates). NC, negative control.

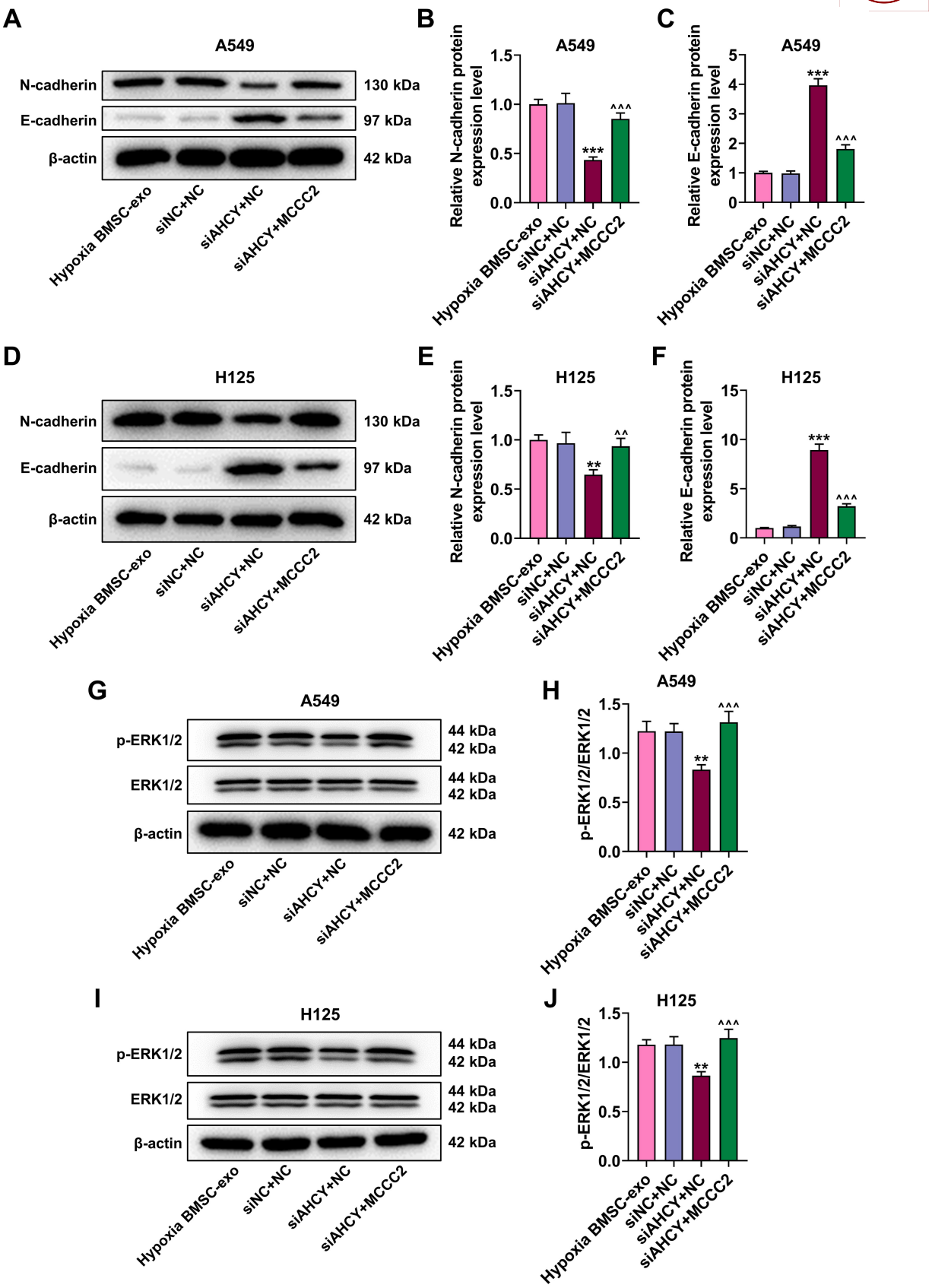

Fig. 8. The effects of siAHCY and MCCC2 overexpression on EMT-related proteins and ERK pathway-related proteins of LC cells. (A–F) N-cadherin and E-cadherin expressions in LC cells (Western blotting, β-actin as internal control). (G–J) ERK1/2 and p-ERK/1/2 expression levels in LC cells (Western blotting, β-actin as internal control). $^{**}p < 0.01$, $^{***}p < 0.001$ vs. siNC+NC. $^{\wedge\wedge}p < 0.01$, $^{\wedge\wedge\wedge}p < 0.001$ vs. siAHCY+NC. The experiments were triplicate (n = 3 biological replicates).

to confirm the AHCY-MCCC2 regulatory axis. Thirdly, the mechanism by which AHCY regulates MCCC2 remains to be further clarified, particularly whether it involves methylation regulation of MCCC2. Finally, this study has not been validated in animal experiments, and such *in vivo* investigations are needed in the future.

Conclusions

In a word, this study showed that hypoxia BMSC-exo transmits AHCY to LC cells through intercellular communication, resulting in high expression of MCCC2 in LC cells, which further leads to the activation of ERK1/2 in LC cells and promotes the malignant development of LC cells. Our findings may provide promising avenues for optimizing LC treatment strategies.

Availability of Data and Materials

The analyzed data sets generated during the study are available from the corresponding author on reasonable request.

Author Contributions

BH and FM designed the research study; JH performed the research; ZZ and CS collected and analyzed the data; XS made substantial contributions to conception, design, and drafting of the manuscript. All authors have been involved in revising it critically for important intellectual content. All authors gave final approval of the version to be published. All authors have participated sufficiently in the work to take public responsibility for appropriate portions of the content and agreed to be accountable for all aspects of the work in ensuring that questions related to its accuracy or integrity.

Ethics Approval and Consent to Participate

Not applicable.

Acknowledgment

Not applicable.

Funding

This research received no external funding.

Conflict of Interest

The authors declare no conflict of interest.

Supplementary Material

Supplementary material associated with this article can be found, in the online version, at https://doi.org/10.24976/Discov.Med.202638208.128.

References

[1] Nooreldeen R, Bach H. Current and Future Development in Lung Cancer Diagnosis. International Journal of Molecular Sciences. 2021; 22: 8661. https://doi.org/10.3390/ijms22168661.

[2] Hirsch FR, Scagliotti GV, Mulshine JL, Kwon R, Curran WJ, Jr, Wu YL, *et al*. Lung cancer: current therapies and new targeted treatments. Lancet (London, England). 2017; 389: 299–311. https://doi.org/10.1016/S0140-6736(16)30958-8.

[3] Sun J, Wu S, Jin Z, Ren S, Cho WC, Zhu C, *et al*. Lymph node micrometastasis in non-small cell lung cancer. Biomedicine & Pharmacotherapy. 2022; 149: 112817. https://doi.org/10.1016/j.biopha.2022.112817.

[4] Li MY, Liu LZ, Dong M. Progress on pivotal role and application of exosome in lung cancer carcinogenesis, diagnosis, therapy and prognosis. Molecular Cancer. 2021; 20: 22. https://doi.org/10.1186/s12943-021-01312-y.

[5] Xu K, Zhang C, Du T, Gabriel ANA, Wang X, Li X, *et al*. Progress of exosomes in the diagnosis and treatment of lung cancer. Biomedicine & Pharmacotherapy. 2021; 134: 111111. https://doi.org/10.1016/j.biopha.2020.111111.

[6] Lan T, Luo M, Wei X. Mesenchymal stem/stromal cells in cancer therapy. Journal of Hematology & Oncology. 2021; 14: 195. https://doi.org/10.1186/s13045-021-01208-w.

[7] Ding W, Zhang K, Li Q, Xu L, Ma Y, Han F, *et al*. Advances in Understanding the Roles of Mesenchymal Stem Cells in Lung Cancer. Cellular Reprogramming. 2023; 25: 20–31. https://doi.org/10.1089/cell.2022.0133.

[8] Vakhshiteh F, Atyabi F, Ostad SN. Mesenchymal stem cell exosomes: a two-edged sword in cancer therapy. International Journal of Nanomedicine. 2019; 14: 2847–2859. https://doi.org/10.2147/IJN.S200036.

[9] Zhang X, Sai B, Wang F, Wang L, Wang Y, Zheng L, *et al*. Hypoxic BMSC-derived exosomal miRNAs promote metastasis of lung cancer cells via STAT3-induced EMT. Molecular Cancer. 2019; 18: 40. https://doi.org/10.1186/s12943-019-0959-5.

[10] Ancel J, Perotin JM, Dewolf M, Launois C, Mulette P, Nawrocki-Raby B, *et al*. Hypoxia in Lung Cancer Management: A Translational Approach. Cancers. 2021; 13: 3421. https://doi.org/10.3390/cancers13143421.

[11] Chengcheng L, Raza SHA, Shengchen Y, Mohammedsaleh ZM, Shater AF, Saleh FM, *et al*. Bioinformatics role of the WGCNA analysis and co-expression network identifies of prognostic marker in lung cancer. Saudi Journal of Biological Sciences. 2022; 29: 3519–3527. https://doi.org/10.1016/j.sjbs.2022.02.016.

[12] Kobayashi S, Zimmermann H, Millhorn DE. Chronic hypoxia enhances adenosine release in rat PC12 cells by altering adenosine metabolism and membrane transport. Journal of Neurochemistry. 2000; 74: 621–632. https://doi.org/10.1046/j.1471-4159.2000.740621.x.

[13] Chen YY, Zhang XN, Xu CZ, Zhou DH, Chen J, Liu ZX, *et al*. MCCC2 promotes HCC development by supporting leucine oncogenic function. Cancer Cell International. 2021; 21: 22. https://doi.org/10.1186/s12935-020-01722-w.

[14] Ishola AA, Chien CS, Yang YP, Chien Y, Yarmishyn AA, Tsai PH, *et al*. Oncogenic circRNA C190 Promotes Non-Small Cell Lung Cancer via Modulation of the EGFR/ERK Pathway. Cancer Research. 2022; 82: 75–89. https://doi.org/10.1158/0008-5472.CAN-21-1473.

[15] Liu X, Jiang F, Wang Z, Tang L, Zou B, Xu P, *et al*. Hypoxic bone marrow mesenchymal cell-extracellular vesicles containing miR-328-3p promote lung cancer progression via the NF2-mediated Hippo axis. Journal of Cellular and Molecular Medicine. 2021; 25: 96–109. https://doi.org/10.1111/jcmm.15865.

[16] Ling F, Yang W, Yuan M, Chen Y, Li J, Wu J, *et al*. Delivery of bone marrow mesenchymal stem cell-derived exosomes into fibroblasts attenuates intestinal fibrosis by weakening its transdifferentiation via the CCN2-TGF-β axis. Scientific Reports. 2025; 15: 18048. https://doi.org/10.1038/s41598-025-02971-3.

[17] Vizán P, Di Croce L, Aranda S. Functional and Pathological Roles of AHCY. Frontiers in Cell and Developmental Biology. 2021; 9: 654344. https://doi.org/10.3389/fcell.2021.654344.

[18] Wang J, Ding K, Wang Y, Yan T, Xu Y, Deng Z, *et al*. Wumei Pill Ameliorates AOM/DSS-Induced Colitis-Associated Colon Cancer through Inhibition of Inflammation and Oxidative Stress by Regulating S-Adenosylhomocysteine Hydrolase- (AHCY-) Mediated Hedgehog Signaling in Mice. Oxidative Medicine and Cellular Longevity. 2022; 2022: 4061713. https://doi.org/10.1155/2022/4061713.

[19] Park SJ, Kong HK, Kim YS, Lee YS, Park JH. Inhibition of S-adenosylhomocysteine hydrolase decreases cell mobility and cell proliferation through cell cycle arrest. American Journal of Cancer Research. 2015; 5: 2127–2138.

[20] Gupta A, Storey KB. Coordinated expression of Jumonji and AHCY under OCT transcription factor control to regulate gene methylation in wood frogs during anoxia. Gene. 2021; 788: 145671. https://doi.org/10.1016/j.gene.2021.145671.

[21] Tong L. Structure and function of biotin-dependent carboxylases. Cellular and Molecular Life Sciences: CMLS. 2013; 70: 863–891. https://doi.org/10.1007/s00018-012-1096-0.

[22] Dai W, Feng H, Lee D. MCCC2 overexpression predicts poorer prognosis and promotes cell proliferation in colorectal cancer. Experimental and Molecular Pathology. 2020; 115: 104428. https://doi.org/10.1016/j.yexmp.2020.104428.

[23] Liu Y, Yuan Z, Song C. Methylcrotonoyl-CoA carboxylase 2 overexpression predicts an unfavorable prognosis and promotes cell proliferation in breast cancer. Biomarkers in Medicine. 2019; 13: 427–436. https://doi.org/10.2217/bmm-2018-0475.

[24] He J, Mao Y, Huang W, Li M, Zhang H, Qing Y, *et al*. Methylcrotonoyl-CoA Carboxylase 2 Promotes Proliferation, Migration and Invasion and Inhibits Apoptosis of Prostate Cancer Cells Through Regulating GLUD1-P38 MAPK Signaling Pathway. OncoTargets and Therapy. 2020; 13: 7317–7327. https://doi.org/10.2147/OTT.S249906.

[25] Sugiura R, Satoh R, Takasaki T. ERK: A Double-Edged Sword in Cancer. ERK-Dependent Apoptosis as a Potential Therapeutic Strategy for Cancer. Cells. 2021; 10: 2509. https://doi.org/10.3390/cells10102509.

[26] Olea-Flores M, Zuñiga-Eulogio MD, Mendoza-Catalán MA, Rodríguez-Ruiz HA, Castañeda-Saucedo E, Ortuño-Pineda C, *et al*. Extracellular-Signal Regulated Kinase: A Central Molecule Driving Epithelial-Mesenchymal Transition in Cancer. International Journal of Molecular Sciences. 2019; 20: 2885. https://doi.org/10.3390/ijms20122885.